Fish and Shellfish Immunology 89 (2019) 505–515

Contents lists available at ScienceDirect

Fish and Shellfish Immunology

journal homepage: www.elsevier.com/locate/fsi

Full length article

De novo assembly, characterization of tissue-specific transcriptomes and identification of immune related genes from the scallop *Argopecten purpuratus*

Patricio Flores-Herrera[a,1], Rodolfo Farlora[b,1], Roxana González[a], Katherina Brokordt[c], Paulina Schmitt[a,*]

[a] Grupo de Marcadores Inmunológicos, Laboratorio de Genética e Inmunología Molecular, Instituto de Biología, Facultad de Ciencias, Pontificia Universidad Católica de Valparaíso, Chile
[b] Laboratorio de Biotecnología Acuática y Genómica Reproductiva, Instituto de Biología, Facultad de Ciencias, Universidad de Valparaíso, Chile
[c] Laboratory of Marine Physiology and Genetics (FIGEMA), Centro de Estudios Avanzados en Zonas Áridas (CEAZA) and Universidad Católica Del Norte, Chile

A B S T R A C T

The scallop *Argopecten purpuratus* is one of the most economically important cultured mollusks on the coasts from Chile and Peru but its production has declined, in part, due to the emergence of mass mortality events of unknown origin. Driven by this scenario, increasing progress has been made in recent years in the comprehension of immune response mechanisms in this species. However, it is still not entirely understood how different mucosal interfaces participate and cooperate with the immune competent cells, the hemocytes, in the immune defense. Thus, in this work we aimed to characterize the transcriptome of three tissues with immune relevance from *A. purpuratus* by next-generation sequencing and *de novo* transcriptome assembly. For this, 18 cDNA libraries were constructed from digestive gland, gills and hemocytes tissues of scallops from different immune conditions and sequenced by the Illumina HiSeq4000 platform. A total of 967.964.884 raw reads were obtained and 967.432.652 clean reads were generated. The clean reads were *de novo* assembled into 46.601 high quality contigs and 32.299 (69.31%) contigs were subsequently annotated. In addition, three *de novo* specific assemblies were performed from clean reads obtained from each tissue cDNA libraries for their comparison. Gene ontology (GO) and KEGG analyses revealed that annotated sequences from digestive gland, gills and hemocytes could be classified into both general and specific subcategory terms and known biological pathways, respectively, according to the tissue nature. Finally, several immune related candidate genes were identified, and the differential expression of tissue-specific genes was established, suggesting they could display specific roles in the host defense. The data presented in this study provide the first insight into the tissue specific transcriptome profiles of *A. purpuratus*, which should be considered for further research on the interplay between the hemocytes and mucosal immune responses.

1. Introduction

The scallop *Argopecten purpuratus* is one of the most economically important cultured bivalve mollusk on the coasts from Chile and Peru [1]. Nevertheless, its production has declined in recent years due, in part, to the emergence of mass mortality events. The causes of these mortalities are still not well known but they have been associated with bacteria from the genus *Vibrio* in larvae [2]. In addition, several species of scallops are facing mortalities events in China and Europe, which are likely due to bacterial pathogens [3–5]. Scallop culture is subjected to a high population density and large fluctuation of environmental conditions, which can affect the animal immune function, increasing the possibility of succumbing to diseases. Therefore, it is essential to elucidate the diverse immune response mechanisms of this bivalve to develop protocols for the management of infections and to design efficient strategies to prevent and control infectious outbreaks.

Molluscan defense is based mainly on innate immune mechanisms mediated by the immune competent cells, the hemocytes, and humoral defense factors [6]. In this context, significant progress has been made in the comprehension of immune response mechanisms of hemocytes in bivalve mollusks [7]. As all invertebrates, scallop hemocytes can recognize the non-self, using pattern recognition receptors [8] and soluble proteins [9] (PRRs/PRPs) which lead to the activation of signaling pathways. This activation promotes the synthesis of immune effectors that could mediate the recruitment of other hemocytes, activate the phagocytic process and produce antimicrobial molecules [7,10]. Several genes involved in signaling cascades and immune effectors have been characterized from *A. purpuratus* hemocytes [11–13]. Yet, most important host-microbe interactions may occur at the mucosal interfaces, and there is little information about how different epithelia

* Corresponding author.
E-mail address: paulina.schmitt@pucv.cl (P. Schmitt).
[1] both authors contributed equally to this work.

https://doi.org/10.1016/j.fsi.2019.03.069
Received 28 January 2019; Received in revised form 26 March 2019; Accepted 28 March 2019
Available online 30 March 2019

participate and cooperate with the hemocytes in the immune defense [10]. Considering that the first contact with pathogens occurs at the epithelial surfaces, mucosal factors could have a prominent role in bivalve immunity and resistance to infections. Then, it is necessary to characterize the immune response at the epithelial level, considering that the achievement of the pathogenic infection depends on great extent in the primary interaction with the host; which could be intense on filter-feeders such as bivalves.

In the last years, transcriptomic high throughput sequencing of organisms has been widely recognized to be an efficient method for gene discovery and analysis of differential gene expression [14]. Furthermore, this technology has been extremely helpful for the study of non-model organisms for which genomes are not sequenced. Nowadays, a growing number of transcriptomic data from bivalves are available from mussels, clams, oysters [15] and scallops, such as *A. irradians* [16] *Chlamys nobilis* [17], *C. farreri* [18], *Patinopecten yessoensis* [19] and *Pecten maximus* [4,20]. Nevertheless, no transcriptomic data from high throughput sequencing are available at present in *A. purpuratus*, besides one draft genome that has just been published [21]. Hence, the availability of an annotated transcriptome from *A. purpuratus* will provide new baselines for functional genomic approaches.

Virtually all infectious diseases are initiated at epithelial surfaces and to the best of our knowledge, no comparative analyses of tissue specific transcriptomes including mucosal barriers are found in scallops. Only few studies are found in other marine invertebrates, such as starfish [22] sea urchin [23], and clam [24,25]. In this context, comparing different tissues possessing immune/internal defense features from *A. purpuratus* by transcriptome analysis will provide a systemic notion of their interaction, which is required for a functional understanding of scallop immune response. The aim of this study is to characterize the transcriptome of digestive gland, gills and hemocytes from *A. purpuratus* by high throughput sequencing and *de novo* transcriptome assembly. Here, we describe the transcriptome of the scallop with a special focus on the tissue specific immune transcript profile of immune related genes.

2. Materials and methods

2.1. Sample collection

US National Research Council guidelines for the care and use of laboratory animals were strictly followed during this research. Sixty adult scallops (65 ± 5 mm shell height) aged between 14 and 16 months with immature gonads, were sampled from the aquaculture facilities of the Universidad Católica del Norte (UCN) located at the Tongoy bay, Chile (30°16′ S, 71° 35′W). In order to include tissues with variable immune status in the analysis, 100 µL of heat-killed *Vibrio splendidus* VPAP16 in 0.22 µm filtered sea water (FSW) (1×10^6 cells/scallop) or 100 µL of FSW, as injury control, were injected in the adductor muscle of 20 scallops per condition. Twenty non-injected scallops were also included. Scallops were returned to the lantern net and maintained at the sea aquaculture facilities (water temperature: 13 °C, depth: 5–10 m). After 24 h, the 60 scallops were collected and transferred to the laboratory at the UCN, Coquimbo, Chile. Hemolymph was collected individually from the pericardial cavity and hemocytes were isolated by centrifugation (600 × *g* for 5 min at 4 °C). 20 pieces of gills and digestive gland tissues (3–4 mm^3 each) from the same 20 scallops per condition were harvested by dissection under sterile conditions. Samples from the three tissues were kept in TRizol at −80 °C until total RNA extraction.

2.2. RNA extraction and library construction

Total RNA was extracted from *A. purpuratus* tissues using TRIzol® reagent according to manufacturer instructions (Thermo Scientific). RNA was then treated with DNAse I (Thermo Scientific), 15 min at room temperature and inactivated by heat, 10 min at 65 C, followed by a second precipitation with sodium acetate 0.3 M (pH 5.2) and isopropanol (1:1 v:v). The quantity and quality of total RNA were assessed using a TapeStation 2200 (Agilent Technologies Inc) using the RNA ScreenTape according to the manufacturer's instructions. To validate the activation of the immune response by the Vibrio injection, cDNA was synthesized from hemocytes RNA and the gene expression of the antimicrobial peptide ApBD1 was confirmed by qPCR as previously described [12]. After the corroboration of the immune activation, only samples with RIN > 8.0 were used for library preparation using the TruSeq RNA Sample Preparation Kit v2 (Illumina®). For this, three tissues (digestive gland, gills and hemocytes), three conditions (non-injected, FSW injected and heat-killed *Vibrio* injected scallops), and two replicates (2 pools of 10 scallops each) were considered for the construction of 18 cDNA libraries in total.

2.3. High-throughput transcriptome sequencing, de novo assembly and functional annotation

The 18 cDNA libraries were sequenced by the HiSeq4000 (Illumina®) platform using sequenced runs of 2 × 100 paired-end reads at Macrogen, Korea. The raw data for each pool of samples were separately trimmed and *de novo* assembled using the CLC Genomics Workbench software v11.0.0 (CLC Bio). Four *de novo* assemblies were performed using datasets: sequences from the 18 libraries, and from the 6 libraries from each tissue separately. For each assembly, the overlap settings used were a mismatch cost of 2, deletion cost of 3, insert cost of 3, minimum contig length of 500 base pairs, and trimming quality score of 0.05.

National Center for Biotechnology Information (NCBI) non-redundant (NR) Protein and UniprotKB/SwissProt databases were used to annotate the assembled contigs through tBLASTx with a cut off E-value of $1e^{-10}$. The assembled contigs were also annotated according to Gene Ontology terms (GO) and Kyoto Encyclopedia of Genes and Genomes (KEGG) pathways through the Database for Annotation, Visualization and Integrated Discovery (DAVID) 6.8 version and categorized based on GO terms for biological processes, molecular functions, and cellular components, with an e-value cut off of $1e^{-5}$, a minimum sequence filter of 40, and sorted based on level 2 GO classifications. Venn diagrams were constructed from the obtained data showing number of overlapping and non-overlapping categories and pathways in each tissue using Venny software version 2.1.

2.4. Differential expression and clustering analyses

For the RNA-seq expression analysis, the consensus sequences single file generated by the *de novo* assembly using the 18 libraries was used as a reference. The readings from each tissue/condition replicate were separately mapped against this reference transcriptome (46.601 contigs) using the CLC Genomics Workbench software. The RNA-seq settings used were a minimum length fraction of 0.8 and a minimum similarity fraction (long reads) of 0.9. The expression values were set as reads per kilobase of transcript per million mapped reads (RPKM). To identify the differential expression between the analyzed tissues, the differential expression for RNA-seq tool included in the CLC Genomics Workbench software was used. Further on, the differentially expressed transcripts ($|\log2 \text{ fold change}| \geq 4$; false discovery rate (FDR) p-value < 0.05 using the T-test) were visualized in a hierarchical clustering heatmap, with Euclidean distance and complete linkage set as parameters for the analysis.

In order to gain insight into the immune response in *A. purpuratus*, a gene panel composed of sequences putatively involved in immunity was established from the assembled transcriptome. Using the bioinformatic mining of sequences showing significant homologies to immune related genes in the NR protein database (E-value < 0.005), 234 contigs potentially involved in immunity were selected. Then, sequences were

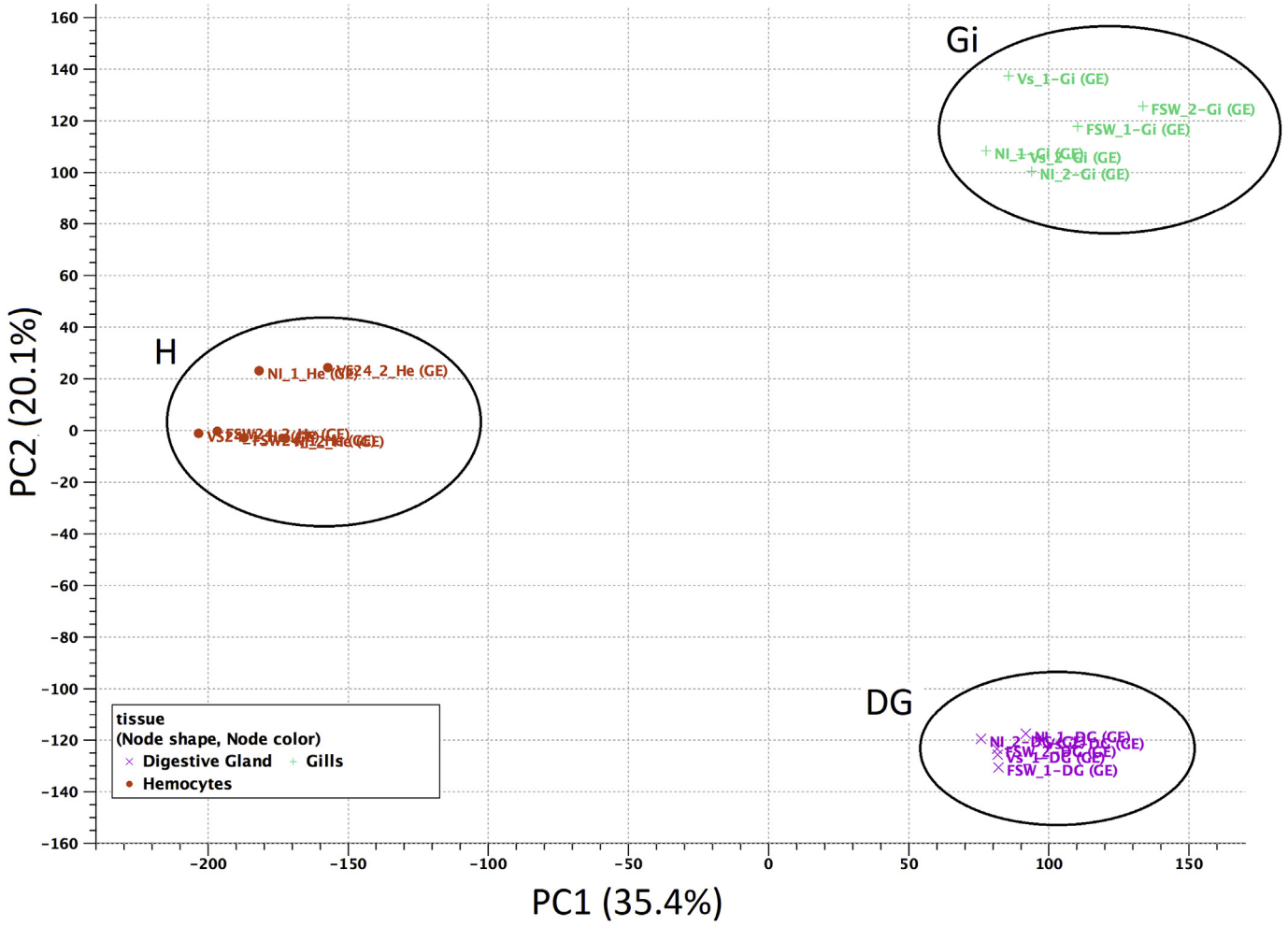

Fig. 1. Principal component analysis (PCA) of the paired-end hemocytes, gills and digestive gland cDNA libraries. Each symbol represents an individual cDNA library. Six libraries per tissue were included in the analysis. DG: digestive gland, Gi: gills, H: hemocytes.

classified into different immune associated categories, such as pattern recognition receptors and proteins, signaling and regulated secretory pathways, lysosome associated molecules, immune related enzymes, and stress-response molecules and antimicrobial effectors. The panel construction criteria considered the functional classification of sequences rather than their presence in tissues. The immune-related gene panel was used as a reference, and the readings from every tissue/condition replicate were separately mapped against it with the CLC Genomics Workbench software using the same RNA-seq settings and hierarchical clustering parameters as described above.

2.5. Data deposition

All the raw reads were submitted to the sequence reads archive (SRA), NCBI database with an accession number of PRJNA494400.

2.6. Validation of gene expression by real-time quantitative PCR (RT-qPCR)

To validate the gene expression of selected immune related genes identified by the RNA-seq analysis, the same RNA used for the construction of the cDNA libraries were used for RT-qPCR amplification. For this, collected RNA from a subset of animals that have been used for the construction of cDNA libraries were used. Thus, RNA from the tissues of three pools of 5 scallops each were chosen for cDNA synthesis using 1 µg of RNA and an AffinityScript qPCR cDNA synthesis kit (Stratagene) according to the manufacturer's instructions.

For the qPCR, the 10 µl-volume reaction consisted in 1 × Brilliant III SYBR Green QPCR master mix (Stratagene), 0.5 µM of each primer and 1 µL of cDNA diluted at 1/5 in sterile ultra-pure water. Primers are listed in Supplementary File S1. RT-qPCR assays were performed in triplicate in a Biorad C1000 Touch Thermocycler CFX96, and primer pair efficiencies (E) were calculated from six serial dilutions of pooled cDNA for each primer pair according to the equation: $E = 10^{[-1/slope]}$. Only primers with E between 95% and 105% were considered. Assays were submitted to an initial denaturation step of 10 min at 95 °C followed by an amplification of the target cDNA (40 cycles of denaturation at 95 °C for 5 s, annealing at 58 °C for 5 s and extension time at 60 °C for 15 s) and fluorescence detection. After an initial 10 s denaturation step at 95 °C, a melting curve was obtained from a start temperature of 65 °C to a final temperature of 95 °C, with an increase of 0.06 °C/s. Relative expression was calculated using the -2^{DDCq} method [26] using the measured quantification cycle (Cq) values of the constitutively expressed gene β-actin (GenBank no. ES469330) to normalize the measured Cq values of target genes.

2.7. Statistical analyses

Principal Component Analysis (PCA) was performed on normalized counts per million (CPM) values from the paired-end digestive gland, gills and hemocytes cDNA library samples, and were plotted onto the two-dimensional space spanned by the first and second principal components of the covariance matrix. For the RNA-seq analysis, the T-test with corrected p-value with the false discovery rate was used,

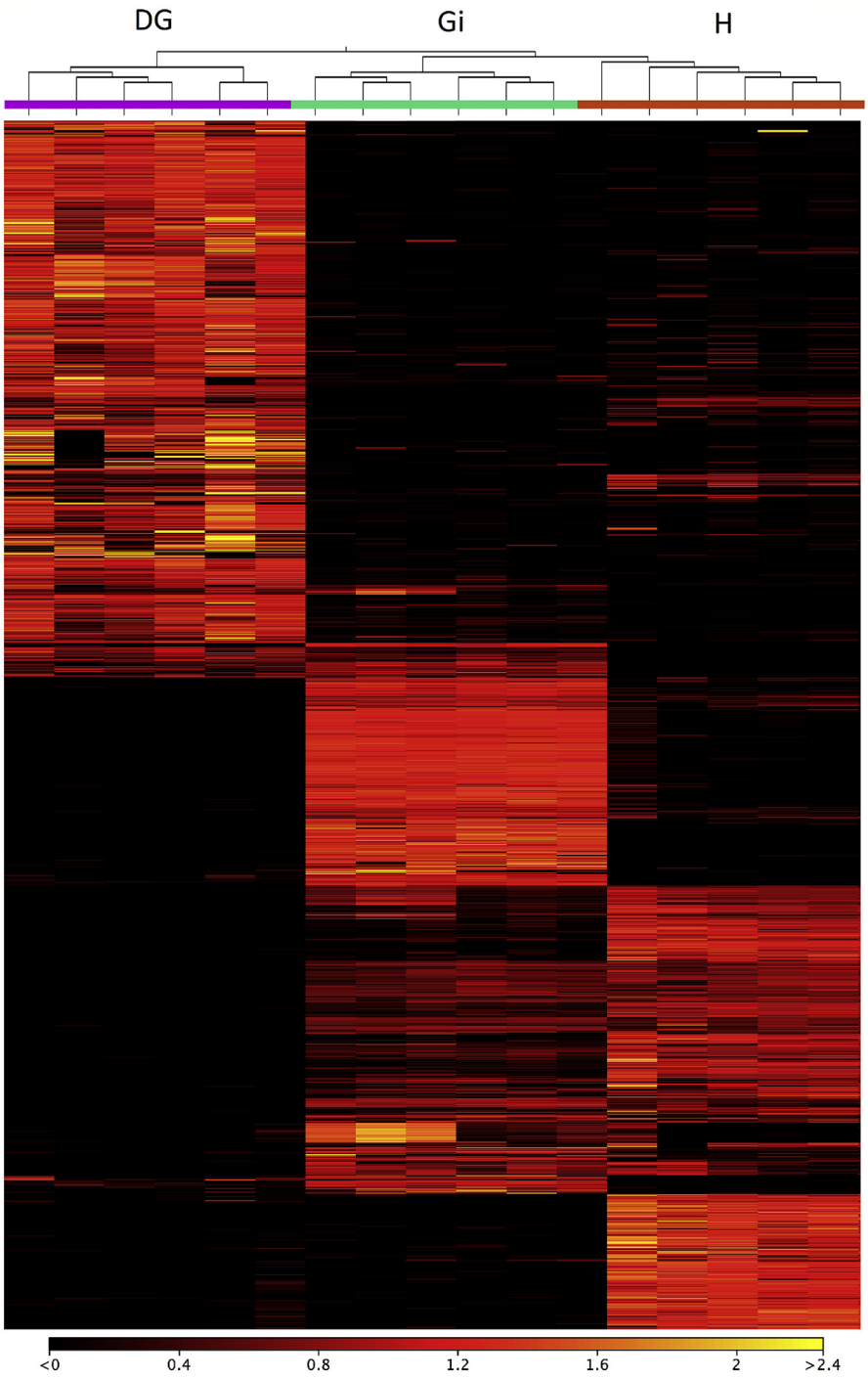

Fig. 2. Hierarchical clustering of differentially expressed genes (DEGs) from digestive gland (DG, purple bar) gills (Gi, green bar) and hemocytes (H, orange bar) transcriptomes from *A. purpuratus*. DEGs were determined with a minimum |log2 fold change| ≥ 4; false discovery rate (FDR) p-value < 0.05 and values are represented through the color scale from black (relative low level of gene expression) to yellow (relative high level of gene expression). (For interpretation of the references to color in this figure legend, the reader is referred to the Web version of this article.)

included in the CLC Genomics Workbench software. Statistical difference between conditions were based on the independent filtering consisting in a cut-off value of log2 ≥ 4 fold change and then, statistical analyses were performed on this subset of filtered transcripts by using selection criteria of p-value < 0.05. For qPCR expression analysis, calculations of means, standard deviations and statistical analysis using Kruskal-Wallis test were carried out using GraphPad Prism software version 6.01 (significant p-value < 0.05).

3. Results

3.1. De novo assembly and differential expression analysis

A total of 18 cDNA libraries from digestive gland, gills and hemocytes tissues RNA were constructed to create a full reference transcriptome of *A. purpuratus* and to assess tissue-specific expression of genes. For this, six libraries per tissue from a pool of scallops presenting different immune status were considered to enrich for both constitutive and regulated tissue-specific immune related transcripts. After quality trimming and the removal of adapters, the sequence runs corresponding to pools of tissues produced a total of 967,432,652 clean reads. In addition, three *de novo* specific assemblies were performed from clean

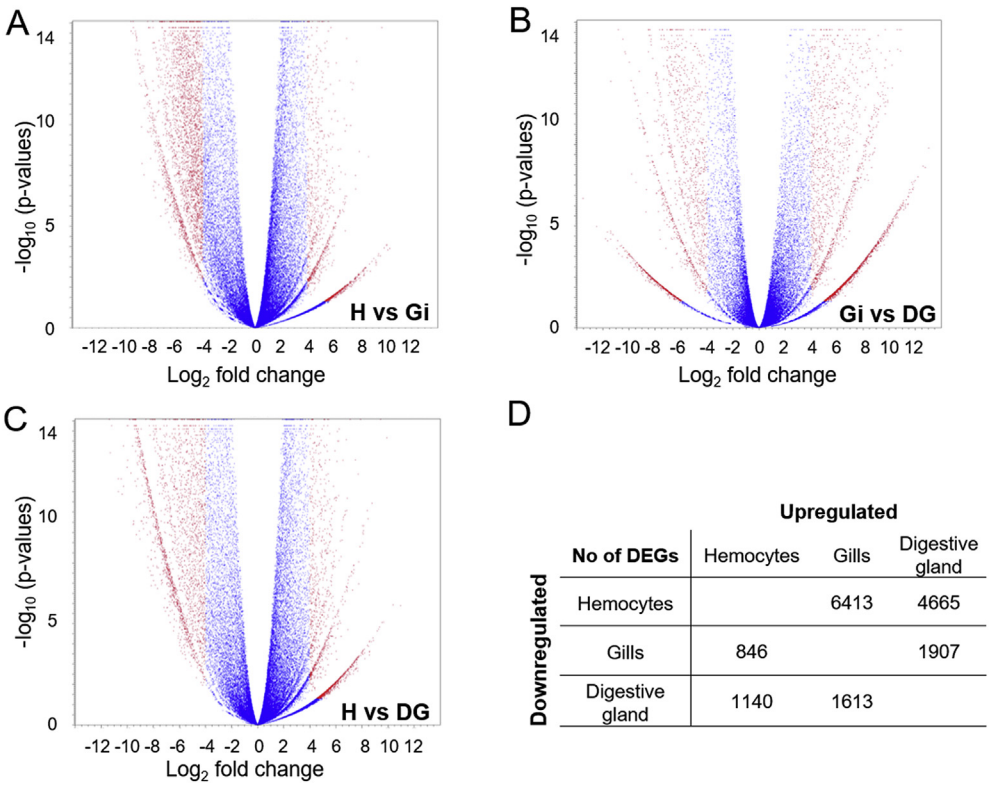

Fig. 3. Volcano plots (panels A–C) from significant differentially expressed genes (DEGs) determined from pair-wise comparisons between **A.** hemocytes vs gills, **B.** gills vs digestive gland and **C.** hemocytes vs digestive gland transcriptomes. Statistically significant transcripts are shown by |log2 fold change| ≥ 4 vs -log10 (p-value) in red. **D.** Statistics of up and downregulated significant DEGs among the three analyzed tissues. (For interpretation of the references to color in this figure legend, the reader is referred to the Web version of this article.)

reads obtained from each tissue cDNA libraries. For hemocyte, gills and digestive gland samples, a total number of 483,519,728; 237,096,646 and 246,816,278 clean reads were produced respectively. The total number of contigs generated by the three *de novo* assemblies from hemocyte, gills and digestive gland reads was 34,977; 34,200 and 30,494 respectively. The sequence data generated in this study have been deposited at SRA (Short Read Archive) database under Experiment Accession PRJNA494400. The total number of contigs generated by the complete *de novo* assembly was 46,601 with an average length of 1651 bp (Supplementary File S1).

To evaluate the transcriptome similarity between samples, principal component analysis (PCA) (Fig. 1) and hierarchical clustering were performed (Fig. 2). Both analyses revealed three distinct groupings: one group consisting of the six libraries from hemocytes, one group from the digestive gland libraries, and another group from the gill libraries. PCA revealed that the 55.5% of the data was explained by the nature of the analyzed tissue. Accordingly, the samples clustered according to the different tissue types rather than by their immune status (either naïve, injected with FSW or injected with FSW containing heat-killed *V. splendidus*), revealing the specialized nature of their transcriptomes. This result prompted us to deepen the tissue-specific immune profile by an RNA-seq analysis.

The full *de novo* assembly was used as reference to perform a differential expression analysis between digestive gland, gills and hemocytes samples. The significant differentially expressed genes (DEGs) were determined from pair-wise comparisons (|log2 fold change| ≥ 4, FDR p-value 0.05). Overall, 7259 DEGs were detected between hemocytes and gills, 3520 DEGs between gills and digestive gland, and 5805 DEGs between hemocytes and digestive gland (Fig. 3, panels A–C) (Supplementary File S2). Among all comparisons, gills was the tissue that showed the highest number of overexpressed DEGs, with 6413 contigs compared to hemocytes and 1613 contigs compared to digestive gland. The digestive gland showed also a high number of overexpressed DEGs, with 4665 contigs compared to hemocytes and 1907 contigs compared to gills. Hemocytes showed 846 and 1140 overexpressed DEGs compared to gills and digestive gland, respectively (Fig. 3, panel D).

3.2. Functional annotation

Transcripts from the full transcriptome assembly and from each specific tissue transcript assembly were then compared separately to the NBCI NR protein database for functional annotation, using BLASTx with an cut off e-value of $1e^{-10}$. For the full transcriptome assembly, a total of 32.299 (69.31%) contigs showed significant similarity to known proteins in the NR database and therefore, successfully annotated. For the three *de novo* assemblies from digestive gland, gills and hemocytes a total of 23,874 (78.29%), 25,968 (75.92%) and 24,611 (70.36%) contigs were successfully annotated, respectively.

The DAVID gene functional classification tool was used to categorize the functions of the predicted scallop transcripts from each tissue separately. Based on sequence homology, annotated contigs were classified into biological processes, cellular components or molecular functions GO categories (Fig. 4, Supplementary File S3). GO classification revealed that 15,959 (66.85%); 17,019 (65.54%) and 16,414 (66.69%) annotated sequences from digestive gland, gill and hemocytes could be classified into 71, 70 and 70 subcategory terms, respectively. Digestive gland, gills and hemocytes shared 54 (35.3%) subcategory terms, while displaying 22 (14.4%) terms specific to each tissue at the cellular component category; they shared 49 (33.6%) subcategory terms while presenting 25 (17.1%), 20 (13.7) and 21 (14.4%) terms specific to each tissue on the molecular function category. Finally, they shared 93 (25.6%) subcategory terms while showing 56 (15.4%), 58 (16%) and 74 (20.4%) specific terms at the biological processes category for digestive gland, gills and hemocytes, respectively (Fig. 4).

Several subcategory terms where shared among the three tissues at the three functional categories. The largest common terms among the three tissues at the cellular component category were cytoplasm (No of counts between 1091 and 1110, representing 6.53–6.91%), nucleoplasm (633–648, 3.81–3.86%), cytosol (677–701, 4.25–4.27%), and membrane (484–500, 2.84–3.13%) subcategories. Within the molecular function category, the most represented terms shared by the three

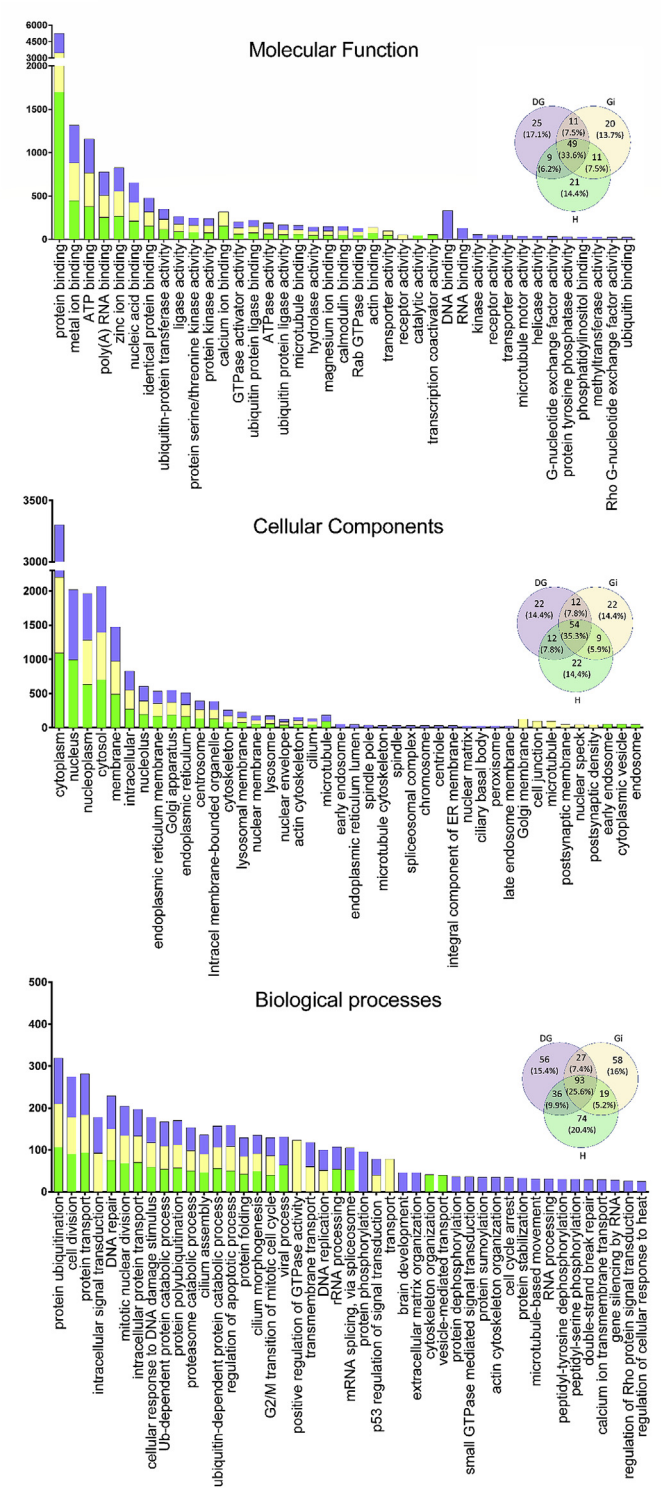

Fig. 4. Distribution of GO terms classification for the annotated contigs from specific tissue transcriptomes from *A. purpuratus*. Stacked bar plots describe the distribution of cellular components, molecular function and biological processes categories in digestive gland (purple bars), gills (yellow bars) and hemocytes (green bars). The size of each bar is proportional to the number of counts classified in each functional subcategory. GO terms were determined using DAVID with an cut off e-value of 10^{-5}, a minimum sequence filter of 40, and sorted based on level 2 GO classifications. Venn diagrams of unique and common transcripts among the three transcriptomes showing the number and percentage of all classified transcripts is included for each category. DG: digestive gland, Gi: gills, H: hemocytes. (For interpretation of the references to color in this figure legend, the reader is referred to the Web version of this article.)

tissues were protein binding (1696–1777, 10.35–11.15%), metal ion binding (432–446, 256–2.71%), ATP binding (379–393, 2.27–2.46%) and poly(A) RNA binding (253–271, 1.5–1.7%). At the biological processes category, protein ubiquitination (106–123, 0.65–0.72%), cell division (90–97, 0.54–0.61%), protein transport (93–97, 0.57–0.61%) and DNA repair (75–79, 0.45–0.50%) showed the higher representation in the three tissues (Fig. 4, Supplementary File S3).

Certain specific subcategories were only found shared by two tissues. For instance, only hemocytes and digestive gland sequences were classified for viral process (64–67; 0.39–0.42%), rRNA processing (53–54; 0.32–0.33%) and mRNA splicing (52–53; 0.31–0.33%) at the biological processes category. In the molecular function category, only hemocytes and gills transcripts were classified into the GO terms calcium ion binding (153–162; 0.93–0.95%), actin binding (67–70; 0.39–0.42%) and transporter activity (47–51; 0.28–0.31) (Fig. 4, Supplementary File S3). Finally, several annotated sequences from each analyzed tissue were classified into single particular terms. For instance, only hemocytes transcripts were classified in early endosome (51, 0.31%), cytoplasmic vesicle (51, 0.31%) and endosome (49, 0.29%) from cellular components; catalytic (44, 0.26%) and transcription coactivator (55, 0.33%) activity from molecular function, and cytoskeleton organization (41, 0.25%) and vesicle-mediated transport (40, 0.2%) from biological processes (Fig. 4, Supplementary File S3).

The KEGG database was further used to assess the biological interaction of scallop genes from each tissue separately. A total of 601 (3.77%), 542 (3.19%) and 512 (3.13%) annotated sequences from digestive gland, gills and hemocytes respectively showed significant matches in the KEGG database. These sequences were assigned to 24, 22 and 19 known biological pathways (Fig. 5, Supplementary File S4). Digestive gland, gills and hemocytes annotated sequences shared 16 KEGG pathways (55.2%), while sharing 1 pathway (6.9%) between hemocytes and digestive gland sequences, 2 pathways (6.9%) between gills and digestive gland sequences and no shared pathways between hemocytes and gills sequences. Sequences from each tissue were also classified in single pathways, displaying 5 (17.2%), 3 (10.3%) and 2 (6.9%) pathways for digestive gland, gills and hemocytes respectively. (Fig. 5).

The most represented common pathways were ubiquitin mediated proteolysis (hsa04120), protein processing in endoplasmic reticulum (hsa04141), purine metabolism (hsa00230), RNA transport (hsa03013) and lysosome (hsa04142), with more than 40 counts on every tissue. As observed by DAVID functional classification, transcripts from single tissues were specifically classified in particular pathways, such as protein digestion and absorption (hsa04974), galactose metabolism (hsa00052) and pantothenate and CoA biosynthesis (hsa00770) for digestive gland sequences; *N*-Glycan biosynthesis (hsa00510) and DNA replication (hsa03030) for gills sequences, and glyoxylate and dicarboxylate metabolism (hsa00630) and glycine, serine and threonine metabolism (hsa000260) for hemocytes sequences (Supplementary File S4).

3.3. Identification of immune related candidate genes and assessment of tissue specific differential expression

An exhaustive examination of the full annotated transcriptome from *A. purpuratus* was performed to identify candidate genes that might be functionally associated with immunity. By the bioinformatic mining of sequences showing significant homologies to immune related genes in the NR protein database (E-value < 0.005), 234 contigs potentially involved in immunity were selected. Then, they were classified into different immune associated categories, such as pattern recognition receptors and proteins, signaling and regulated secretory pathways, lysosome associated molecules, immune related enzymes, and stress-response molecules and antimicrobial effectors (Supplementary File S5).

The selected panel of immune related sequences was used as a

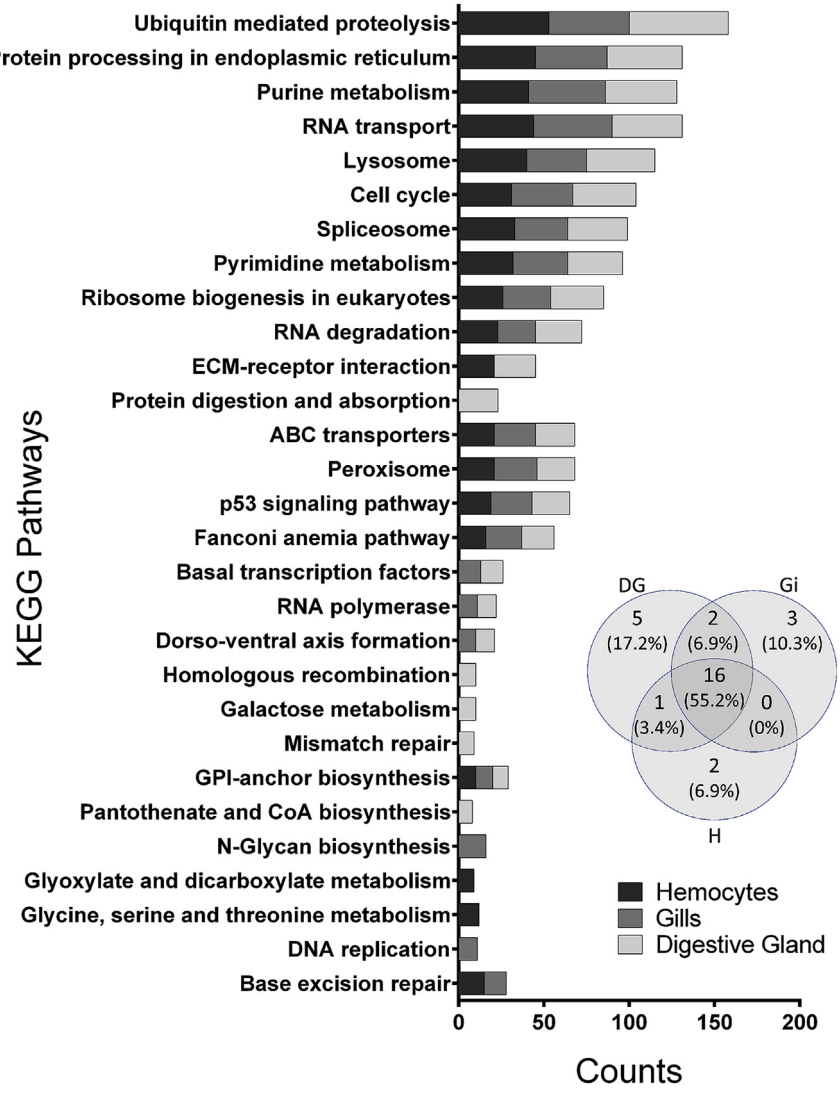

Fig. 5. Tissue specific categorization of *A. purpuratus* transcriptomes to KEGG biochemical pathways. A KEGG biochemical pathway analysis was performed on hemocytes, gills and digestive gland transcriptomes. The stacked bars represent the top 29 KEGG pathways and their distribution in each tissue, using an cut off e-value of 10^{-5} and minimum pathway assignment cut off of 8. A Venn diagram of unique and common pathways among the three transcriptomes is included showing the number and percentage of categorized transcripts. DG: digestive gland, Gi: gills, H: hemocytes.

reference to assess their differential expression among digestive gland, gills and hemocytes (Supplementary file S6). Results showed a total of 49 DEGs from the immune panel between hemocytes and gills, 85 DEGs between gills and digestive gland and 78 DEGs between hemocytes and digestive gland. 65 overexpressed DEGs were detected in digestive gland compared to hemocytes and 59 overexpressed DEGs in digestive gland compared to gills. Gills showed 38 and 26 overexpressed DEGs compared to hemocytes and digestive gland respectively. Finally, hemocytes showed 11 and 13 overexpressed DEGs compared to gills and digestive gland respectively (Supplementary file S6). A hierarchical clustering was then constructed from this RNA-seq analysis data. The resulting heatmap showed a specific expression profile of the immune related candidate genes, which could be grouped in three distinct clusters (Fig. 6). Specifically, contigs from the cluster 1 was mostly overexpressed in hemocytes, contigs from cluster 2 in digestive gland and contigs from cluster 3 in gills. Then, the representation of the different immune associated categories in each cluster were assessed. Cluster 1 gathered contigs from every category in a well-balanced manner, with a major occurrence of immune signaling pathways related sequences (31.6%), followed by lysosome related molecules (20.2%) and immune related enzymes (19.4%). Cluster 2 showed an overrepresentation of PRRs and PRPs candidate genes (33.6%) and immune signaling pathways (28.1%) with the lowest incidence of immune related enzymes (8%). Finally, cluster 3 showed high representation of stress-response and antimicrobial effectors (25.6%) followed by immune related enzymes and lysosome related molecules (respectively 24.6 and 23.8%) and to a lesser extent immune signaling pathway related molecules (Fig. 6).

Finally, the top 10 overexpressed contigs in each tissue was determined by pairwise comparisons from the differential expression analysis data (Table 1). The top 10 contigs overexpressed specifically in hemocytes correspond to PRRs only (Fig. 6, cluster 1), including lectins, mannose receptors and binding proteins and Toll-like receptors (TLRs). The contigs found to be overexpressed specifically in the digestive gland, compared to hemocytes and gills were PRRs (C-type lectin and Beta-glucan binding protein) but also antimicrobial effectors, such as MPEG-1 and Complement C1q-like proteins (Fig. 6, cluster 2). In gills, the most overexpressed contigs compared to hemocytes and digestive gland were two PRRs corresponding to a TLR and a scavenger receptor (CD163 antigen like protein), and a protein from the interleukins (IL) family, specifically an IL-17 like protein (Fig. 6, cluster 3). Thus, results highlight the specialized nature of PRRs and effector molecules for each

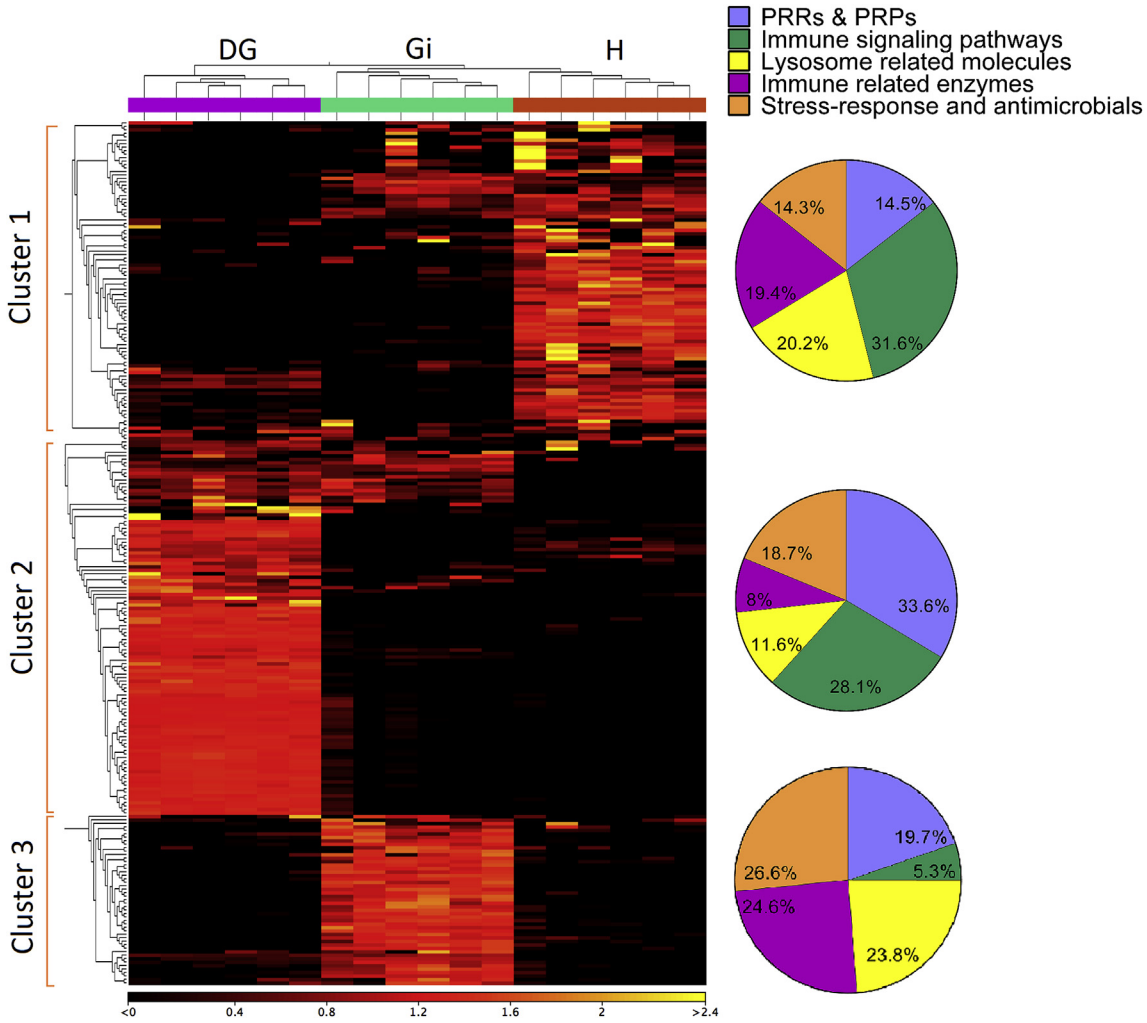

Fig. 6. Hierarchical clustering of a subset of 234 immune related transcripts from digestive gland (DG, purple bar), gills (Gi, green bar) and hemocytes (H, orange bar) from *A. purpuratus*. DEGs were determined with a minimum |log2 fold change| ≥ 4; false discovery rate (FDR) p-value < 0.05, and values are represented through the color scale from black (relative low level of gene expression) to yellow (relative high level of gene expression). At left, clusters associated to a specific tissue are showed by square brackets (1; hemocytes; 2: digestive gland; 3: gills). At right, pie charts showing the proportion of different immune associated categories in each cluster. (For interpretation of the references to color in this figure legend, the reader is referred to the Web version of this article.)

scallop tissue.

3.4. Validation of tissue-specific expression of immune related genes by RT-qPCR

Finally, six specific transcripts highly overexpressed in one tissue compared to the two others were selected for RT-qPCR analysis and validation of the RNA-Seq results (Table 1). Thus, transcripts encoding for a mannose receptor-like protein, a C-type lectin, a complement C1q-like protein, a macrophage expressed gene-1 (MPEG-1), an interleukin 17- like protein (IL-17) and a scavenger receptor (CD163 antigen like-1) were selected as candidates for tissue-specific immune markers. The RT-qPCR analysis validated the RNA-seq results, showing that the C1q transcript was overexpressed in the digestive gland and the MPEG-1 transcript was found predominantly expressed in digestive gland and to a lesser extent in gills, transcripts encoding a scavenger receptor and the IL-17 was principally detected in gills while the C-type lectin and a mannose receptor-like protein were specifically overexpressed in circulating hemocytes (Fig. 7, panel A). Furthermore, the expression values (log2 fold change) from the RNA-seq were compared to those derived from the RT-qPCR analysis (Fig. 7, panel B). As expected, the fold change value was consistent between methods, supported by the correlation analysis (R^2: 0.90).

4. Discussion

Transcriptome sequencing has been proposed as an efficient method for gene discovery and analysis of differential gene expression in non-model organisms [22]. The draft genome of *Argopecten purpuratus* has been only recently published [21] but still, genome assemblies of non-model species can be compromised by high levels of polymorphism as observed in the oyster *Crasssostrea gigas* [27]. Thus, the availability of annotated transcriptomes from different tissues of species like *A. purpuratus* could serve as a platform to guide future functional genomic approaches.

Results from PCA revealed that transcripts were not categorized according to treatments but rather according to tissues. Hence, first we aimed to carry out a comparative study between tissues to obtain a broad assessment of their specific transcriptomes, that could highlight specific features in the scallop immune response. Therefore, total clean reads from the tissues and from every experimental group were included in the whole *de novo* assembly to cover as many sequences that could be expressed in scallops from different immune status. A considerable proportion of the obtained transcripts showed high identities with protein sequences on the public protein database. High identities indicated the accuracy of the contigs obtained by the next-generation sequencing and *de novo* transcriptome assembly. Still, 30.69% of

Table 1
Top 10 DEGs within each cluster from the hierarchical clustering constructed by the immune panel RNA-seq analysis (hemocytes, cluster 1; digestive gland, cluster 2; gills, cluster 3). In bold, tissue-specific overexpressed genes from each cluster.

Cluster	Top 10 Contigs	Log_2 FC	FDR	Acc. No	Description
	Overexpressed in H vs DG				
HEMOCYTES	contig_0009276	6473	4,64E-10	P02707	Hepatic lectin
	contig_0001401	5158	0	Q7TSQ1	Mannose receptor-like protein
	contig_0000012	6139	0	Q9NR16	CD163 antigen-like 1
	contig_0000241	6121	0	Q9QZ15	C-type lectin
	contig_0000512	4583	0	Q9V477	Toll-like receptor 8
	contig_0003948	4466	4,02E-16	Q0PV50	Toll-like receptor 3
	contig_0000889	4440	0	Q66S60	Mannose-binding protein
	contig_0029967	6342	0,000053	A1E295	Cathepsin B
	contig_0018802	4772	0	Q6EIG7	C-type lectin
	contig_0005601	5828	0	P42930	Heat shock protein beta-1
	Overexpressed in H vs Gi				
	contig_0009276	5,7773	2,56E-08	P02707	Hepatic lectin
	contig_0001401	6,1581	0	Q7TSQ1	Mannose receptor-like protein
	contig_0000012	5,8142	0	Q9NR16	CD163 antigen-like 1
	contig_0000241	5,8977	0	Q9QZ15	C-type lectin
	contig_0000512	5,0841	0	Q9V477	Toll-like receptor 8
	contig_0003948	4,2185	3,71E-14	Q0PV50	Toll-like receptor 3
	contig_0000889	4,2970	0	Q66S60	Mannose-binding protein
	contig_0005832	4,3622	2,64E-10	P15941	Mucin-1
	contig_0009244	4,3209	0	Q9QZ15	C-type lectin
	contig_0002649	4,5626	0	Q4ZJM9	Complement C1q-like protein
	Overexpressed in DG vs H				
DIGESTIVE GLAND	contig_0037050	12,231	3,30E-09	Q9ESN4	Complement C1q-like protein
	contig_0041010	11,554	0	Q86Z23	Complement C1q-like protein
	contig_0046031	11,775	0	Q5RBP9	MPEG-1
	contig_0030195	11,963	0	A7X413	C-type lectin
	contig_0040977	10,782	0	Q8N0N3	Beta-1,3-glucan-binding protein
	contig_0043699	11,963	0	Q90WJ8	Lactose-binding lectin
	contig_0030433	12,345	0	Q2V459	Putative defensin-like protein
	contig_0045828	12,179	0	B3A003	Lysozyme
	contig_0043764	11,002	2,13E-07	B3A003	Lysozyme
	contig_0038239	10,957	0	G9JJU2	Glutathione peroxidase
	Overexpressed in DG vs Gi				
	contig_0037050	8374	0	Q9ESN4	Complement C1q-like protein
	contig_0041010	10,328	0	Q86Z23	Complement C1q-like protein
	contig_0045016	12,615	0,0004	Q5RBP9	MPEG-1
	contig_0042891	9028	0	Q8IUN9	C-type lectin
	contig_0040977	7335	0	Q8N0N3	Beta-1,3-glucan-binding protein
	contig_0045000	8744	9,73E-07	P98092	Humoral lectin
	contig_0045173	8088	0	P30204	Macrophage scavenger receptor
	contig_0017524	7576	0	Q08420	Extracellular SOD Cu-Zn
	contig_0046557	7451	0	Q66S03	Galactose-specific lectin
	contig_0041181	7421	0	Q4ZJM9	Complement C1q-like protein
	Overexpressed in Gi vs H				
GILLS	contig_0036604	6282	5,57E-07	Q9NR97	Toll-like receptor 8
	contig_0046256	8923	0,00005	Q9NR16	CD163 antigen-like 1
	contig_0044959	6300	7,60E-13	A9XE49	Interleukin 17-like protein
	contig_0046084	8089	0,00017	Q9EPQ1	Toll/IL-1 receptor-like protein
	contig_0024781	8915	0,00005	P49946	Ferritin H
	contig_0024213	6211	0	A2TF48	MyD88
	contig_0039879	6122	0	Q68Y56	Toll-like receptor 4
	contig_0043232	5851	0,01	P82756	Putative defensin-like protein
	contig_0045828	5612	1,38E-06	B3A003	Lysozyme 3
	contig_0046031	5503	2,90E-08	Q5RBP9	MPEG-1
	Overexpressed in Gi vs DG				
	contig_0036236	7,3164	3,20E-09	Q9NR97	Toll-like receptor 8
	contig_0046256	5,9240	3,90E-07	Q9NR16	CD163 antigen-like 1
	contig_0044959	6,0633	1,10E-09	A9XE49	Interleukin 17-like protein
	contig_0032602	7,4565	3,36E-09	Q13478	Interleukin-18 receptor 1
	contig_0037079	9,0945	4,54E-12	Q704V6	Toll-like receptor 6
	contig_0032962	6,9279	1,11E-11	Q685J3	Small intestinal mucin-3
	contig_0045335	6,7959	4,10E-16	P10716	C-type lectin
	contig_0027457	6,4735	0	Q14162	Scavenger receptor class F
	contig_0033653	6,4389	4,23E-07	Q704V6	Toll-like receptor 6
	contig_0028589	8,5609	3,68E-11	Q9DGB6	Toll-like receptor 2

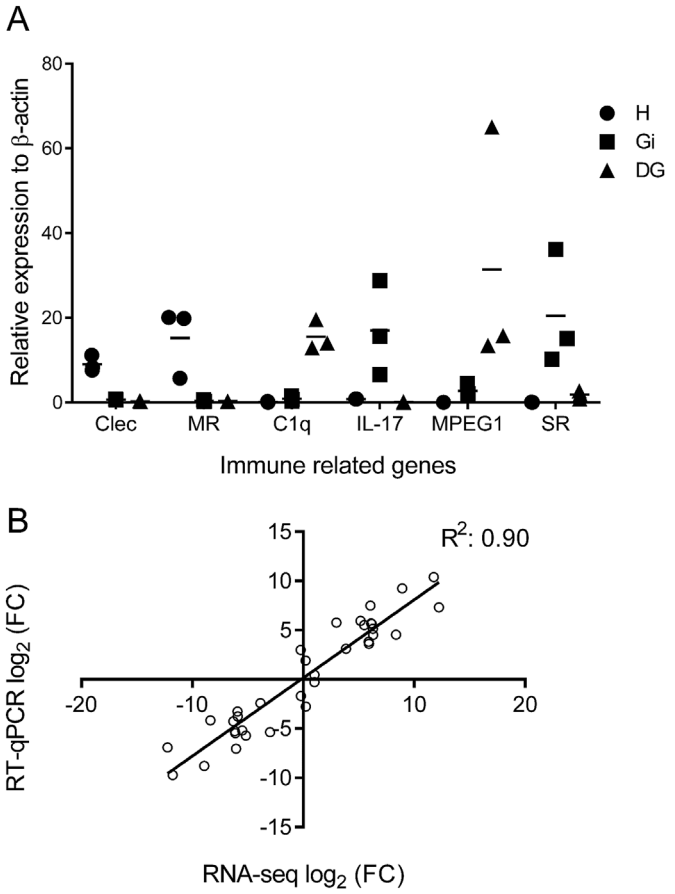

Fig. 7. RT-qPCR validation of RNA-seq results. **A.** Relative expression of six scallop immune related genes in digestive gland, gills and hemocytes tissues obtained by RT-qPCR according to the $2^{-\Delta\Delta Cq}$ method. The scallop β-actin gene was used as reference gene. Results are expressed as single dots from 3 pools of 5 scallops per tissue. Mean values are indicated by a straight line. Clec: C-type lectin; MR: mannose receptor; C1q: Complement 1q protein; IL-17: interleukin 17-like protein; MPEG1: macrophage expressed gene 1; SR: scavenger receptor (CD163 like protein) **B**. Correlation analysis between RNA-seq and RT-qPCR log2 fold change results from pairwise comparisons among tissues from the same RNA samples. R^2: Spearman Correlation coefficient.

transcripts were not annotated, suggesting the lack of similar sequences in public databases from phylogenetically closest species.

The high level of similarity between the main subcategories of GO terms among the three tissues could be interpreted as tissues sharing several common functionalities. However, it could be also explained by the limited bivalve information in public protein databases, which is reflected in the about 35% of annotated contigs not considered in the classification, a feature also reported in transcriptomic analyses from other non-model organisms [19,23,28]. Nonetheless, in the present study GO analysis also revealed certain tissue-specific GO subcategories, highlighting particular functions related to the tissues. For instance, the terms cytoskeleton organization and vesicle-mediated transport from the biological processes category were only spotted in hemocytes. One of the central hallmarks of these mobile cells is their phagocytic capacity and the cytoskeleton organization and vesicle-mediated transport are essential steps in this process [29,30]. Furthermore, the predicted tissue-specific functions obtained by KEGG analysis, which only consisted in about 4% of the annotated contigs, fits coherently with the nature of each tissue, such as protein digestion and absorption for digestive gland, a tissue that plays a central role in protein metabolism [31] or DNA replication in gills, a tissue which is currently proposed as an hematopoietic site in mollusks [32]. Therefore, functional characterization of molluscan tissues can still be obtained by these bioinformatic tools due to the conserved nature of protein domains. Yet, much is remaining to be done to characterize the functional relevance of those neglected contigs, and next-generation sequencing will help as a powerful tool, increasing the coverage of the extensive molluscan diversity [33].

A differential expression of genes among tissues, both global and according to the immune related panel of genes was detected by the RNA-seq analyses. The tissue showing the highest number of DEGs was the gills when compared to hemocytes and digestive gland. This result could reflect the diversity of cell types present in this complex tissue, which is one of the most exposed epithelia of bivalves, fulfilling gas exchange and filter feeding functions [34]. Also, the potential overlapping with the transcriptome of the infiltrating hemocytes cannot be rule out, which could further increase the number of DEGs in gills when comparing to circulating hemocytes. Nevertheless, it is tempting to speculate that different mucosal interfaces such as gills cooperate with the infiltrating hemocytes through the maintenance of the homeostasis and during an immune response. Indeed, the synergistic effects of antimicrobial effectors expressed in hemocytes and epithelia have been shown in the oyster *C. gigas* [35] and this type of functional interplay might also occur in scallops.

The RNA-seq analysis from the immune gene panel sequences showed the differential expression of certain genes according to the tissue, suggesting they could display specific roles in the host defense. Hemocytes seem to overexpress a high proportion of PRRs/PRPs such as lectins (soluble and membrane bound), a scavenger receptor (CD163 antigen-like 1) and Toll-like receptors. Hemocytes are responsible for the recognition of the non-self, the first and crucial step in the maintenance of immune homeostasis and thus, those recognition molecules could serve as both, sentinels and cell markers. Gills, on the counterpart, seem to overexpress some PRRs but also an IL17-like protein. This cytokine-like molecule has been characterized recently in oysters, where it activates immune signaling pathways and display antibacterial and microbe associated with molecular patterns binding [36]. Thus, existence of soluble immune-regulatory molecules in scallops such as IL-17, and the possibility of a cytokine-like signaling network in mollusks, definitely adds complexity to the innate immune system [37]. Digestive gland overexpresses PRRs as well but also it expresses the highest proportion of antimicrobial effectors, such as macrophage-expressed gene 1 (MPEG1) and complement C1q-like proteins. MPEG-1 is an integral membrane protein with a predicted membrane attack complex/perforin domain associated with host defense against invading pathogens [38]. C1q is the protein which initiates the classical complement pathway mediating a variety of immunoregulatory functions [39]. The digestive gland is an organ related to digestion metabolisms, but many crucial genes involved in immunity are reported to be expressed in this tissue [40]. Therefore, it is plausible that transcriptomic changes measured in the current study denote signatures of tissue-specific immune features, as well as the expression of hemocyte infiltrating immune genes despite the low number of analyzed replicates. Now, the validation of the tissue-specific expression of the genes in other scallops and from different immune status will allow improvements on the systemic notion of their interactions, and a better understanding of the complexity of the immune response. The most relevant host-microbe interactions may occur at the mucosal interfaces, and there is little information about mucosal immune factors and how different epithelia participate and cooperate with the hemocytes in the immune defense [10]. Thus, in a next step, the evaluation of the expression of the different genes specific to each tissue during a stronger and pathogenic immune challenge may provide greater evidence of how they interact for an effective defense.

5. Conclusion

In conclusion, we have documented a *de novo* transcriptome analysis from digestive gland, gills and hemocytes tissues from the scallop

A. purpuratus. We have identified several immune related genes and results have shown a specific nature of these genes to each tissue, suggesting a more complex contribution of mucosal interfaces on the immune response of scallops than previously thought. In the future, studies comparing the tissue-specific immune responses after a pathogenic challenge will help unveiling the complexity of the hemocyte-mucosal surfaces crosstalk during infections.

Acknowledgments

We gratefully acknowledge Germán Lira from Laboratorio Central de Cultivos from UCN for scallop procurement and maintenance, and Dr. Rodrigo Rojas for bacteria procurement. This study was supported by CONICYT-Chile FONDECYT No 11150009 to P.S., R.G and P.F-H. R.G. was also supported by the PhD student fellowship CONICYT-PFCHA/ DOCTORADO NACIONAL/2016–21160980.

Appendix A. Supplementary data

Supplementary data related to this article can be found at https://doi.org/10.1016/j.fsi.2019.03.069.

References

[1] Food and Agriculture Organization of the United Nations, FAO Yearbook. Fisheries and Aquaculture Statistics, (2016).
[2] R. Rojas, C.D. Miranda, R. Opazo, J. Romero, Characterization and pathogenicity of vibrio splendidus strains associated with massive mortalities of commercial hatchery-reared larvae of scallop argopecten purpuratus (Lamarck, 1819), J. Invertebr. Pathol. 124 (2015) 61–69.
[3] C. Lambert, J. Nicolas, Specific inhibition of chemiluminescent activity by pathogenic vibrios in hemocytes of two marine Bivalves : pecten maximus and crassostrea gigas to cite this version : specific inhibition of chemiluminescent activity by pathogenic vibrios in hemocytes of, J. Invertebr. Pathol. 71 (1998) 53–63.
[4] M. Pauletto, M. Milan, R. Moreira, B. Novoa, A. Figueras, M. Babbucci, et al., Deep transcriptome sequencing of pecten maximus hemocytes: a genomic resource for bivalve immunology, Fish Shellfish Immunol. 37 (2014) 154–165.
[5] N. Sandlund, L. Torkildsen, T. Magnesen, S. Mortensen, Ø. Bergh, Immunohistochemistry of great scallop pecten maximus larvae experimentally challenged with pathogenic bacteria, Dis. Aquat. Org. 69 (2006) 163–173.
[6] L. Wang, L. Qiu, Z. Zhou, L. Song, Research progress on the mollusc immunity in China, Dev. Comp. Immunol. 39 (2013) 2–10.
[7] B. Allam, D. Raftos, Immune responses to infectious diseases in bivalves, J. Invertebr. Pathol. 131 (2015) 121–136.
[8] L. Qiu, L. Song, W. Xu, D. Ni, Y. Yu, Molecular cloning and expression of a toll receptor gene homologue from zhikong scallop, chlamys farreri, Fish Shellfish Immunol. 22 (2007) 451–466.
[9] J. Yang, L. Wang, H. Zhang, L. Qiu, H. Wang, L. Song, C-type Lectin in Chlamys farreri (CfLec-1) mediating immune recognition and opsonization, PLoS One 6 (2011) 16–19.
[10] B. Allam, E.P. Espinosa, E. Pales Espinosa, Bivalve immunity and response to infections: are we looking at the right place? Fish Shellfish Immunol. 53 (2016) 4–12.
[11] D. Oyanedel, R. Gonzalez, P. Flores-Herrera, K. Brokordt, R.D. Rosa, L. Mercado, et al., Molecular characterization of an inhibitor of NF-κB in the scallop Argopecten purpuratus: first insights into its role on antimicrobial peptide regulation in a mollusk, Fish Shellfish Immunol. 52 (2016) 85–93.
[12] R. Gonzalez, K. Brokordt, C. Carcamo, T. Coba de la Peña, D. Oyanedel, L. Mercado, et al., Molecular characterization and protein localization of the antimicrobial peptide big defensin from the scallop argopecten purpuratus after vibrio splendidus challenge, Fish Shellfish Immunol. 68 (2017) 173–179.
[13] T. Coba de la Peña, C.B. Cárcamo, M.I. Díaz, K.B. Brokordt, F.M. Winkler, Molecular characterization of two ferritins of the scallop Argopecten purpuratus and gene expressions in association with early development, immune response and growth rate, Comp. Biochem. Physiol. B Biochem. Mol. Biol. 198 (2016) 46–56.
[14] N.M. Dheilly, A. Coen, D.A. Raftos, G. Benjamin, D.P. Louis, No more non-model species: the promise of next generation sequencing for comparative immunology, Dev. Comp. Immunol. 45 (2015) 56–66.
[15] T. Yarra, K. Gharbi, M. Blaxter, L.S. Peck, M.S. Clark, Characterization of the mantle transcriptome in bivalves : pecten maximus, mytilus edulis and crassostrea gigas, Mar. Genom 27 (2016) 9–15.
[16] C. Chi, S.S. Giri, J.W. Jun, H.J. Kim, S.W. Kim, J.W. Kang, et al., Detoxification and immune transcriptomic response of the gill tissue of bay scallop (Argopecten irradians) following exposure to the algicide palmitoleic acid, Biomolecules 8 (2018) 139.
[17] Y. Shi, W. Liu, M. He, Proteome and transcriptome analysis of ovary, intersex gonads, and testis reveals potential key sex reversal/differentiation genes and mechanism in scallop Chlamys nobilis, Mar. Biotechnol. 20 (2018) 220–245.
[18] J. Li, L. Pan, J. Miao, R. Xu, W. Xu, De novo assembly and characterization of the ovarian transcriptome reveal mechanisms of the final maturation stage in Chinese scallop Chlamys farreri, Comp. Biochem. Physiol. Genom. Proteonom. 20 (2016) 118–124.
[19] W. Jiang, F. Lin, J. Fang, Y. Gao, M. Du, J. Fang, et al., Transcriptome analysis of the yesso scallop, patinopecten yessoensis gills in response to water temperature fluctuations, Fish Shellfish Immunol. 80 (2018) 133–140.
[20] M. Pauletto, M. Milan, A. Huvet, C. Corporeau, M. Suquet, J.V. Planas, et al., Transcriptomic features of pecten maximus oocyte quality and maturation, PLoS One 12 (2017) e0172805.
[21] C. Li, X. Liu, B. Liu, B. Ma, F. Liu, G. Liu, et al., Draft genome of the peruvian scallop argopecten purpuratus, GigaScience 7 (2018) 1–6.
[22] C. Kim, H. Go, H. Young, Y. Hun, M.R. Elphick, N. Gyu, Transcriptomics reveals tissue/organ-specific differences in gene expression in the star fish Patiria pectinifera, Mar. Genom 37 (2018) 92–96.
[23] Y. Chen, Y. Chang, X. Wang, X. Qiu, Y. Liu, De novo assembly and analysis of tissue-specific transcriptomes revealed the tissue-specific genes and profile of immunity from Strongylocentrotus intermedius, Fish Shellfish Immunol. 46 (2015) 723–736.
[24] B. Allam, E. Pales, A. Tanguy, F. Jeffroy, C. Le, C. Paillard, Transcriptional changes in manila clam (ruditapes philippinarum) in response to brown ring disease, Fish Shellfish Immunol. 41 (2014) 2–11.
[25] X. Zhao, X. Duan, Z. Wang, W. Zhang, Y. Li, C. Jin, et al., Comparative transcriptome analysis of sinonovacula constricta in gills and hepatopancreas in response to vibrio parahaemolyticus infection, Fish Shellfish Immunol. 67 (2017) 523–535.
[26] M.W. Pfaffl, A new mathematical model for relative quantification in real-time RT-PCR, Nucleic Acids Res. 29 (2001) e45.
[27] G. Zhang, X. Fang, X. Guo, L. Li, R. Luo, F. Xu, et al., The oyster genome reveals stress adaptation and complexity of shell formation, Nature 490 (2012) 49–54.
[28] S. Wang, R. Hou, Z. Bao, H. Du, Y. He, H. Su, et al., Transcriptome sequencing of zhikong scallop (Chlamys farreri) and comparative transcriptomic analysis with yesso scallop (patinopecten yessoensis), PLoS One 8 (2013) e63927.
[29] M.A. Burgos-aceves, C. Faggio, An approach to the study of the immunity functions of bivalve haemocytes : physiology and molecular aspects, Fish Shellfish Immunol. 67 (2017) 513–517.
[30] L. Wang, X. Song, L. Song, The oyster immunity, Dev. Comp. Immunol. 80 (2018) 99–118.
[31] Q. Lyu, W. Jiao, K. Zhang, Z. Bao, S. Wang, W. Liu, Proteomic analysis of scallop hepatopancreatic extract provides insights into marine polysaccharide digestion, Sci. Rep. 6 (2016) 34866.
[32] E. Pila, J. Sullivan, X. Wu, J. Fang, S. Rudko, M. Gordy, et al., Haematopoiesis in molluscs: a review of haemocyte development and function in gastropods, cephalopods and bivalves, Dev. Comp. Immunol. 58 (2016) 119–128.
[33] J.H. Schultz, C.M. Adema, Comparative immunogenomics of molluscs, Dev. Comp. Immunol. 75 (2017) 3–15.
[34] M. Gerdol, Y. Fujii, I. Hasan, T. Koike, S. Shimojo, F. Spazzali, et al., The purplish bifurcate mussel mytilisepta virgata gene expression atlas reveals a remarkable tissue functional specialization, BMC Genomics 18 (2017) 590.
[35] P. Schmitt, J. de Lorgeril, Y. Gueguen, D. Destoumieux-Garzón, E. Bachère, Expression, tissue localization and synergy of antimicrobial peptides and proteins in the immune response of the oyster crassostrea gigas, Dev. Comp. Immunol. 37 (2012) 363–370.
[36] L. Xin, H. Zhang, R. Zhang, H. Li, W. Wang, CgIL17-5, an ancient inflammatory cytokine in Crassostrea gigas exhibiting the heterogeneity functions compared with vertebrate interleukin17 molecules, Dev. Comp. Immunol. 53 (2015) 339–348.
[37] U. Rosani, L. Varotto, M. Gerdol, A. Pallavicini, P. Venier, IL-17 signaling components in bivalves : comparative sequence analysis and involvement in the immune responses, Dev. Comp. Immunol. 52 (2015) 255–268.
[38] E. Benard, P. Racz, J. Rougeot, A. Nezhinsky, F. Verbeek, H. Spaink, et al., Macrophage-expressed perforins Mpeg1 and Mpeg1.2 have an anti-bacterial function in zebrafish, J. Innate Immun. 7 (2015) 136–152.
[39] N. Thielens, F. Tedesco, S. Bohlson, C. Gaboriaud, A. Tenner, C1q: a fresh look upon an old molecule, Mol. Immunol. 89 (2017) 73–83.
[40] B. Kim, D. Ahn, H. Kim, J. Lee, J. Rhee, H. Park, Transcriptome profiling suggests roles of innate immunity and digestion metabolism in purplish Washington clam, Genes Genomics 41 (2019) 183–191.